Int. J. Electrochem. Sci., 12 **(2017)** 6379 – 6392, doi: 10.20964/2017.07.37

International Journal of
ELECTROCHEMICAL
SCIENCE
www.electrochemsci.org

Experimental study and Theoretical Simulations of Some Indolinone Based Mannich Bases as Novel Corrosion Inhibitors for Mild Steel in Acid Solutions

Chitrasen Gupta[1], *Ishtiaque Ahamad*[2], *Ambrish Singh*[3,4,*], *Xihua Xu*[4], *Zhipeng Sun*[4], *Yuanhua Lin* [3,4]

[1] Department of Chemistry, Kutir Post Graduate College, Chakkey, Jaunpur, U.P., India.
[2] Department of Applied Chemistry, Institute of Technology, Banaras Hindu University, Varanasi-221005, India.
[3] State Key Laboratory of Oil and Gas Reservoir Geology and Exploitation, Southwest Petroleum University, Chengdu 610500, China.
[4] School of Materials Science and Engineering, Southwest Petroleum University, Xindu district-610500, Chengdu city, Sichuan province, China.
[*]E-mail: vishisingh4uall@gmail.com; drambrishsingh@gmail.com

Received: 5 April 2017 / *Accepted:* 4 May 2017 / *Published:* 12 June 2017

The adsorption behaviour of three Mannich bases [3-(4-chlorophenylimino)-1-(piperidin-1-ylmethyl)indolin-2-one{M-1}, 3-(4-chlorophenylimino)-1-(morpholinomethyl)indolin-2-one{M-2} and 3-(4-chlorophenylimino)-1-[(dibutylamino)methyl]indolin-2-one{M-3}] on mild steel surface in 1M HCl solution was investigated using electrochemical impedance spectroscopy (EIS), polarization curves, and weight loss techniques. The experimental results showed that all Mannich bases are good inhibitors showing >90% inhibition efficiency. Potentiodynamic polarization measurements showed that all studied inhibitors are mixed type. Further, quantum chemical calculations were carried out and the relations between computed parameters and corrosion inhibition efficiency have been discussed.

Keywords: Electrochemical impedance spectroscopy; Mannich base; Corrosion; Quantum chemical calculations

1. INTRODUCTION

Economic losses due to corrosion of mild steel have raised concern of many countries. Acids are used in many industrial operations such as pickling, cleaning, descaling and oil well acidizing, etc which initiate the corrosion process [1]. Relevance of corrosion inhibitors is the most economical and common method to mitigate electrochemical corrosion. It has been reported that many heterocyclic

compounds containing heteroatoms like N, O, and S are effective inhibitors for the corrosion of steel in acid media [2-5]. The heteroatoms can donate the electrons to the unoccupied d orbitals of the metal and hence can form a suitable barrier for corrosion mitigation. The recent papers by many authors also reported the mannich bases, indolines, benzothiazoles, gemini surfactants, carbamates, ionic liquids, imidazoles, Schiff's bases, benzonitrile, and heterocyclic compounds as good corrosion inhibitors of mild steel [6-19]. The mechanism of corrosion mitigation may vary with factors such as the effect of the molecular structure on the electron density of the functional group and the size of the aromatic and aliphatic portions of the molecule [20, 21].

The interactions between the inhibitor molecules and the metal surfaces can be explained and understood in details by theoretical approaches. These approaches have proved to be a very important tool for studying corrosion inhibition mechanism [22-24]. The inhibition property of a compound has been often correlated with energy of highest occupied molecular orbital (HOMO), lowest unoccupied molecular orbital (LUMO) and its (HOMO-LUMO) gap. It is important to note that other parameters viz., vertical electron affinity (E_A) and molecular singlet–triplet energy gap (ΔE_{STG}) were fundamentally more appropriate to correlate with inhibition property [25].

In continuation of our quest for developing Mannich bases as corrosion inhibitors with high effectiveness and efficiency, the present paper aims to investigate the inhibiting properties of 3-(4-chlorophenylimino)-1-(piperidin-1-ylmethyl)indolin-2-one (M-1), 3-(4-chlorophenylimino)-1-(morpholinomethyl)indolin-2-one (M-2) and 3-(4-chlorophenylimino)-1-[(di-n-butylamino)methyl]indolin-2-one (M-3) on the mild steel in hydrochloric acid solutions using the electrochemical measurements weight loss measurements, and theoretical calculations.

2. EXPERIMENTAL

The composition (wt %) C 0.076, P 0.012, Si 0.026, Mn 0.192, Cr 0.050, Cu 0.135, Al 0.023, Ni 0.050 and balance Fe of mild steel were used for weight loss and electrochemical studies. The samples were mechanically cut into 2.5 cm × 2.0 cm × 0.05 cm dimensions, and then abraded with SiC abrasive papers (600, 800, 1000 and 1200 grit) respectively. The specimens were degreased with acetone, dried at room temperature, and kept in desiccator before their use. For electrochemical measurements, the test electrodes were made of the mild steel specimens of dimension 1.0 cm × 1.0 cm (8.0 cm long) and coated with epoxy resin leaving one surface of area of 1.0 cm^2. The exposed surface was abraded with SiC abrasive paper from 600 to 1200, rinsed in distilled water, degreased with acetone, and dried in room temperature. The corrosive medium was 1M HCl solution prepared from analytical-reagent-grade 37% hydrochloric acid and distilled water.

All Mannich bases were synthesized by the condensation of 3-(4-chlorophenylimino)indolin-2-one with secondary amines (viz., piperidine, morpholine and n-dibutylamine) and 3-(4-chlorophenylimino)indolin-2-one was synthesized by condenstation of isatin with p-chloroaniline. The synthetic route and molecular structures with IUPAC name are given in Figure 1. These Mannich bases are soluble in acidic water and hence stock solutions were made directly in molar hydrochloric acid solution.

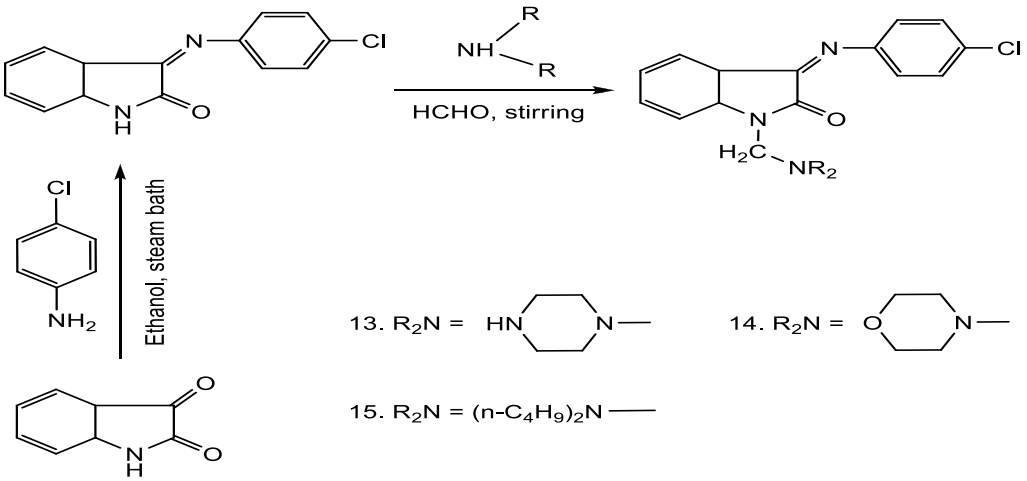

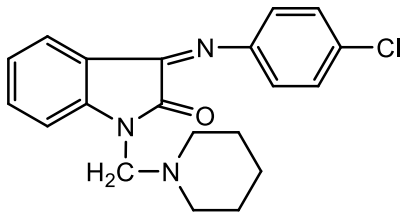

3-(4-chlorophenylimino)-1-(piperidin-1-ylmethyl)indolin-2-one (M-1)

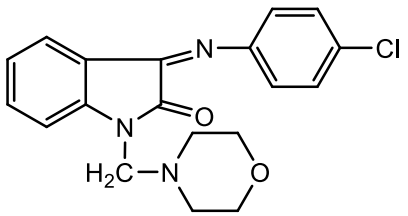

3-(4-chlorophenylimino)-1-(morpholinomethyl) indolin-2-one (M-2)

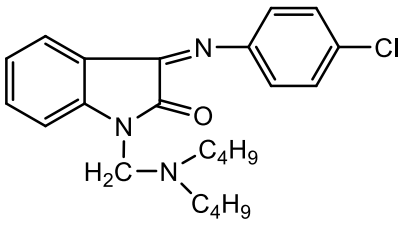

3-(4-chlorophenylimino)-1-[(dibutylamino) methyl]indolin-2-one (M-3)

Figure 1. The synthetic route and molecular structures with IUPAC name of three Mannich bases.

Electrochemical experiments were carried out in a conventional three-electrode glass cell, using a Gamry Potentiostat/Galvanostat–300 electrochemical workstation based on ESA400. A saturated calomel electrode (SCE) equipped with a Luggin capillary and a platinum foil of 1.0 cm × 1.0 cm were used as reference and counter electrode, respectively. Before measurement, the working electrode was immersed in test solution for approximately 1 hour until a steady open-circuit potential (OCP) was reached. EIS measurement was carried out in the 100 kHz to 10 mHz frequency range at

OCP. The polarization curves were carried out using DC 105 software from cathodic potential of -300 mV to anodic potential of +300 mV with respect to the open circuit potential at a sweep rate of 1.0 mV s^{-1}.

Mild steel specimens were immersed in 100 mL of 1M HCl with and without addition of different concentrations of different inhibitors. Weight loss experiment calculated the mean corrosion rate (ρ) as expressed in mg cm^{-2} h^{-1} using following equation:

$$\rho = \frac{\Delta W}{At}$$

where ρ is the average weight loss of three mild steel sheets, A is the total area of one mild steel specimen, and t is the immersion time. With the calculated corrosion rate, the inhibition efficiency (η%) was calculated as follows:

$$\eta\% = \frac{\rho_1 - \rho_2}{\rho_1} \times 100$$

where ρ_1 and ρ_2 are the corrosion rates of the mild steel specimens in the absence and presence of inhibitor, respectively.

Theoretical calculations were carried out at density functional theory (DFT) level using the 6-31G** (d, p) basis set for all atoms with Gaussian 03 W program [26]. For all DFT calculations, the PBE1 functional was used as it has proved its efficiency on a wide range of compounds, and it generally provides accurate results on ground and excited-state properties, including charge-transfer transitions [27].

3. RESULTS AND DISCUSSION

3.1. Electrochemical Impedance Spectroscopy (EIS)

Figure 2a shows the nyquist plots of mild steel in 1M HCl solution in the absence and presence of Mannich bases. The shape of the semicircle obtained does not change while the diameter increases with increase in the concentration of inhibitors. This phenomenon suggested that the corrosion inhibitors adsorbed on the metal surface and the mitigation process followed the same mechanism. Figure 2b and figure 2c represents bode-plot and theta- frequency plots respectively. The inhomogeneity/roughness of the solid surface led to the depressed semicircles with capacitive loop in the high frequency range [28-30]. It is clear that the protection response of metal was modified by the presence of different concentrations of the inhibitor solution. Adsorption of the protective inhibitor layer on the metal surface can also reduce surface heterogeneity and modify its impedance characteristics. The inhibitor molecules adsorbed on the metal surface and decreased the number of exposed active sites that could be involved in metal dissolution. Figure 2d shows the equivalent circuit (R_s, R_{ct}, CPE) used to fit and evaluate all the measured impedance plots. For the description of non-ideal capacitors in the EIS data, a constant phase element (CPE) was used and expressed as [31]:

$$Z_{CPE} = Q^{-1}(j\omega)^{-n}$$

where, ω is the angular frequency, and n is the CPE exponent which can be used as a gauge of the heterogeneity or roughness of the surface [32]. Table 1 show the value of n has a tendency to

increase in presence of inhibitors, which may be attributed to the increase of inhibitor concentration on the metal surface thereby reducing the surface roughness.

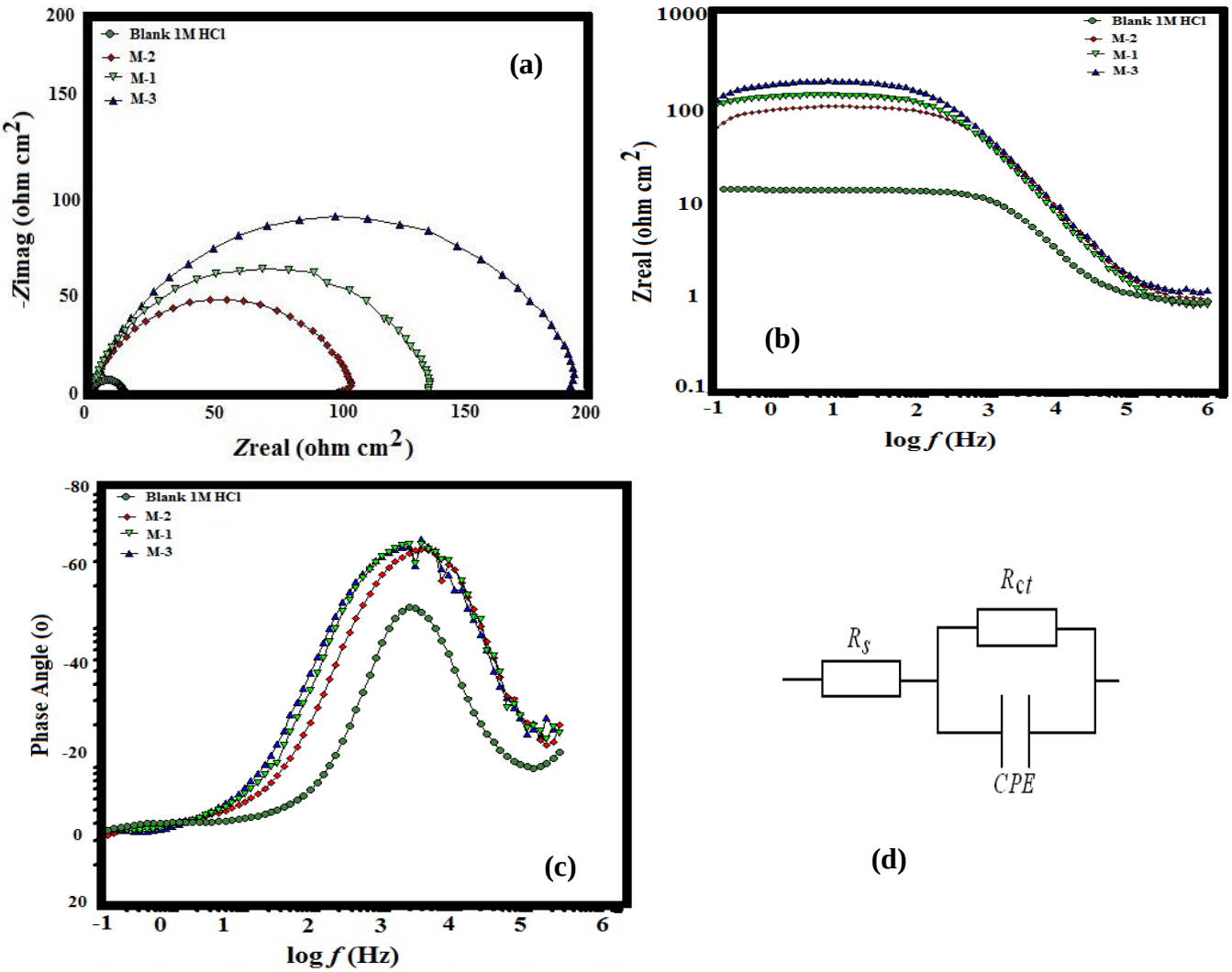

Figure 2. Electrochemical analysis of (a) Nyquist plot (b) Bode plot (c) Theta-frequency plot and (d) Equivalent circuit used for the three mannish base in 1M HCl

For a circuit including a CPE, the C_{dl} could be calculated from CPE parameter values and n using the expression:

$$C_{dl} = Q(\omega_m)^{-n}$$

where C_{dl} is the double layer capacitance and ω_m is the frequency at which the imaginary part of the impedance has a maximum value. The C_{dl} value decreases with increase in concentration as in Table 1 which can be attributed to the adsorption of the inhibitor molecules on the metal surface by replacing the water molecules. This phenomenon leads to the formation of a protective film on metal surface, more the inhibitor is adsorbed, the more the thickness of the barrier layer is increased according to the expression of the Helmholtz model:

$$C_{dl} = \frac{\varepsilon_o \varepsilon}{d} S$$

where d is the thickness of the film, S is the surface area of the electrode, ε_o is the permittivity of the air, and ε is the local dielectric constant. The related inhibitor efficiency was calculated by the charge transfer resistance as follows:

$$\eta_z\% = \frac{R_{t(i)} - R_{t(0)}}{R_{t(i)}} \times 100$$

where $R_{t(i)}$ and $R_{t(0)}$ are the charge transfer resistance in the presence and absence of the inhibitors, respectively.

Table 1. Electrochemical parameters for mild steel in 1M HCl without and with different Mannich bases at 300 mg liter^{-1} concentrations

Inhibitor (300 mg L^{-1})	R_S (Ω cm^2)	R_{ct} (Ω cm^2)	n	Q (10^{-6} Ω^{-1} cm^{-2})	C_{dl} (μF cm^{-2})	η_Z (%)
Blank	0.9	12.2	0.841	281.5	101.2	–
M-1	0.7	130.1	0.843	114.7	51.9	90.6
M-2	0.8	93.5	0.869	132.7	49.2	86.9
M-3	0.9	183.6	0.856	83.4	41.4	93.0

As evident in Table 1, the adsorption of inhibitor molecules on mild steel surface modifies the interface between the corrosive medium and metal surface and decreases its electrical capacity. The decrease in electrical capacity and increase in R_{ct} values in the presence of inhibitors could be interpreted as formation of a protective adsorption layer/film on the electrode surface [33]. Furthermore, to predict the dissolution mechanism, the value of n can be used as an indicator. The values of n, ranging between 0.841 and 0.869, indicate that the charge transfer process controls the dissolution mechanism of mild steel in 1M HCl solution in the absence and in the presence of different inhibitors. Therefore, we can deduce that studied Mannich bases have an obvious role in the metal protection at the concentration of 300 mg L^{-1}.

3.2. Polarization studies

Polarization curves of mild steel in 1M HCl solution without and with different Mannich bases at 300 mg L^{-1} concentration are shown in Figure 3. It could be observed that both the cathodic and anodic reactions were suppressed with the addition of inhibitors, due to the impending inhibitory effect both on anodic dissolution of metal and on cathodic hydrogen reduction reaction. Electrochemical parameters such as E_{corr}, I_{corr}, and anodic and cathodic Tafel slopes (β_a, β_c) obtained from the polarization measurements are listed in Table 2. The inhibition efficiency was calculated by following equation:

$$\eta_P\% = \frac{I_{corr(0)} - I_{corr(i)}}{I_{corr(0)}} \times 100$$

$I_{corr(0)}$ and $I_{corr(i)}$ signify the corrosion current density in the absence and presence of inhibitors, respectively.

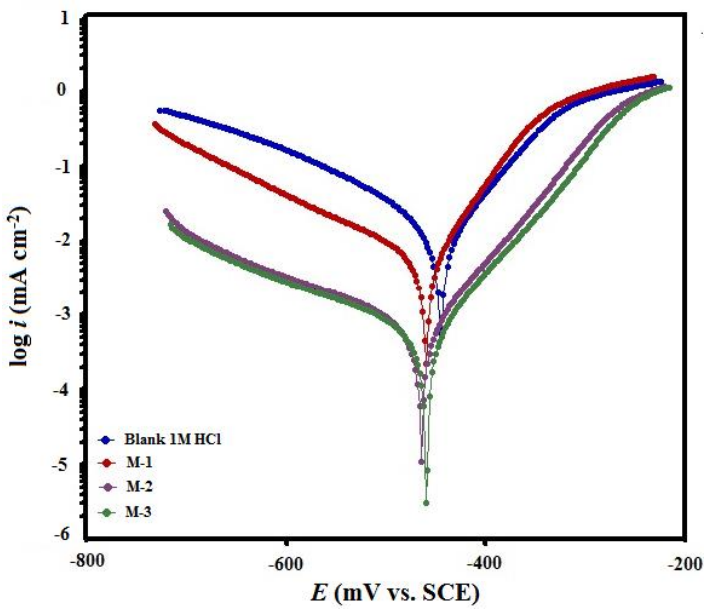

Figure 3. Tafel polarization plot for the three Mannich base in 1 M HCl

As seen from Table 2, addition of inhibitors decreases the corrosion rate of mild steel in 1M HCl. The decrease in corrosion rates in the presence of inhibitors might be due to the adsorption of Mannich bases on the mild steel surface.

Table 2. Polarization parameters for mild steel in 1M HCl without and with different inhibitors at 300 mg liter^{-1} concentrations

Inhibitor	E_{corr}	I_{corr}	b_a	$-b_c$	η_P	C_R
	(mV/SCE)	**(µA cm^{-2})**	**(mV dec^{-1})**	**(mV dec^{-1})**	**(%)**	**(mm year^{-1})**
Blank	-448	1090	85.4	96.6	–	12.7
M-1	-481	124	72.4	119.2	88.6	1.43
M-2	-466	132	73.2	109.2	87.9	1.45
M-3	-472	94	69.3	110.8	91.3	1.10

From these polarization results, it could be seen that the cathodic and anodic curves of the working electrode in the acidic solution containing the inhibitor shifted obviously to the direction of current reduction. The corrosion potential, E_{corr}, value shows a slight shift towards cathodic region and shift in E_{corr} value is 33 mV at maximum. This suggests that all investigated Mannich bases behaved as mixed type inhibitor [34]. The studied inhibitors were first adsorbed onto the metal surface and blocked the reaction sites of the metal surface as suggested by the results [35-40].

3.3. Weight loss measurements

3.3.1. Effect of inhibitor concentration

Corrosion rate (C_R, mm year^{-1}), inhibition efficiency (η%) and weight loss (mg cm^{-2} h^{-1}) obtained from weight loss studies for the mild steel in 1M HCl solution for Mannich bases are listed in Table 3. As can be seen from Table 3 that η% increased and corrosion rate decreased with increasing inhibitor concentration from 50 to 300 mg liter^{-1}. This increased η% and decreased C_R might be due to the result of increased adsorption and increased surface coverage of inhibitor on the mild steel surface while increasing the inhibitor concentration.

Table 3. Corrosion rate of mild steel and inhibition efficiency for different concentrations of Mannich bases in the corrosion of mild steel in 1M HCl obtained from weight loss measurements

Inhibitor	**Concentration (mg L^{-1})**	**C_R (mg cm^{-2} h^{-1})**	**η (%)**
Blank		7.00	–
M-1	50	2.73	60.9
	100	0.87	87.6
	150	0.57	91.9
	200	0.50	92.9
	250	0.47	93.3
	300	0.37	94.8
M-2	50	4.53	35.2
	100	2.37	66.2
	150	1.97	71.9
	200	1.40	80.0
	250	0.93	86.7
	300	0.60	91.4
M-3	50	1.87	73.3
	100	1.23	82.4
	150	0.90	87.1
	200	0.40	94.3
	250	0.30	95.7
	300	0.27	96.2

3.3.2. Effect of temperature

Weight loss measurements were carried out in order to study the effect of temperature on the inhibition performance of M-1, M-2, and M-3 for mild steel in 1M HCl solution in the absence and presence of 300 mg liter^{-1} concentration at temperature ranging from 308 to 338 K for 3 hour exposure time. The results obtained are given in Table 4. It is evident from Table 4 that corrosion rates increased and inhibition efficiencies decreased with increasing the solution temperature from 308 to 338 K. It is also evident from Table 4 that in presence of M-2 C_R increased from 6.7 to 87.9 mm year-1 and η%

decreased from 91.4 to 57.8. The corrosion inhibition of metals by inhibitors in acid solutions largely depends upon two opposite processes adsorption and desorption. When absorption increases, the corrosion rate decreases while inhibition efficiency increases; and if desorption increases, corrosion rate increases while inhibition efficiency decreases. Thus increased corrosion rates in the presence of inhibitors might be due to the increase in desorption with solution temperature. The great increase in C_R and large decrease in % in presence of M-2 can be attributed to more desorption of inhibitor molecules from the mild steel/ solution interface. In this concern, another important parameter the equilibrium adsorption constant (K_a) should be considered.

Table 4. Various corrosion parameters and free energy of adsorption for mild steel in 1M HCl containing 300 mg liter^{-1} Mannich bases at different temperatures

Temp	**1M HCl**	**Inhibitor**											
(K)		**M-1**				**M-2**				**M-3**			
	^aC_R	^aC_R	η %	^aK_a	$^a\Delta G°_a$	^aC_R	η%	^aK_a	$^a\Delta G°_a$	^aC_R	η%	^aK_a	$^a\Delta G°_a$
308	77.9	4.1	94.8	18.41	-35.7	6.7	91.4	10.74	-34.1	3.0	96.2	25.57	-36.3
318	107.6	4.8	95.5	15.28	-36.9	12.2	88.6	7.85	-34.3	6.7	93.8	15.28	-36.1
328	162.5	14.8	90.9	10.09	-36.1	48.9	69.9	2.35	-32.1	17.4	89.3	8.43	-35.6
338	208.5	22.3	89.3	8.43	-36.7	87.9	57.8	1.38	-31.6	33.4	83.9	5.30	-35.4

the values of *CR*, *K* and ΔG^0_a are given in mm year^{-1}, M^{-1} ($\times 10^3$) and kJ mol^{-1}, respectively

It is known that higher the K_a value favours higher adsorption, and smaller K_a value results in lower adsorption. Inspection of Table 4 revealed that K_a values decreased more readily in the presence of M-3 (from 10.74 × 10^3 to 0.26 × 10^3 M^{-1}) with temperature. The values of K_a together with free energy of adsorption ($\Delta G°_a$) support the experimental results. The corrosion rate increases more rapidly with temperature in the absence of the inhibitors than in the presence. These results confirmed that investigated Mannich bases are good inhibitors for the corrosion of mild steel in 1M HCl in the range of temperature under investigation.

3.4. Theoretical calculations

Quantum chemical calculations can be used to support the experimental data such as electrochemical and weight loss by the use of its various parameters [41]. They can also provide molecular-level understanding of the observed experimental behavior.

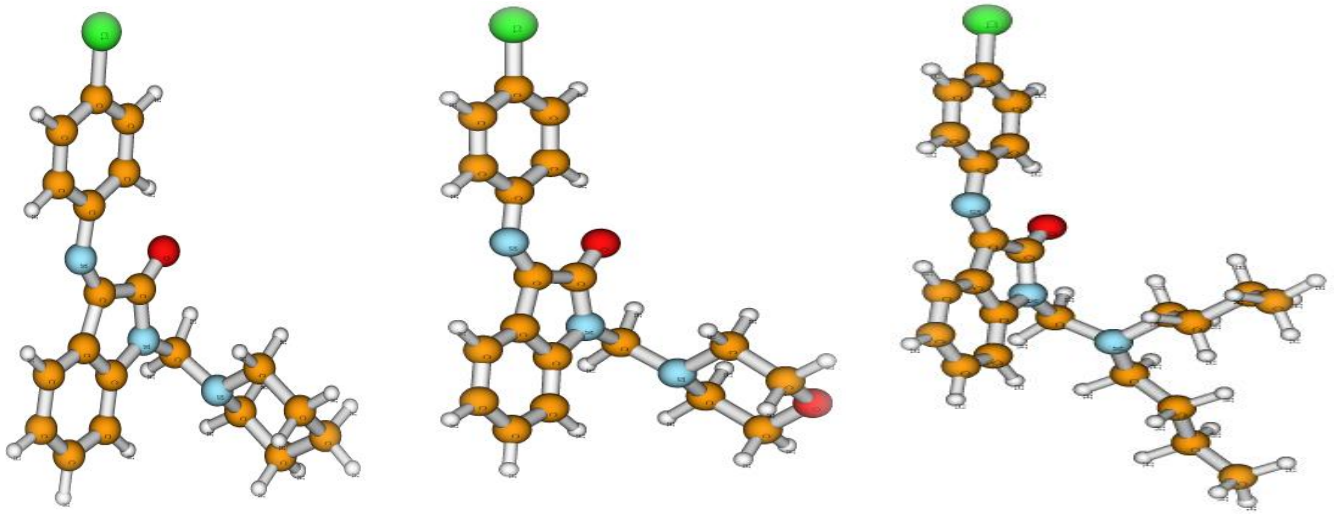

(a) **(b)** **(c)**

Figure 4. Optimized structure of (a) M-1, (b) M-2 and (c) M-2

Table 5 shows some of the computed quantum chemical parameters such as the energies of the highest occupied molecular orbital (E_{HOMO}), lowest unoccupied molecular orbital (E_{LUMO}) and HOMO-LUMO gap (ΔE_{L-H}), vertical electron affinity (EA) and molecular band gap (ΔE_{MBG}). These quantum chemical parameters were obtained after geometric optimization with respect to the all nuclear coordinates using Kohn-Sham approach at DFT level. The fully optimized structures of Mannich bases are shown in figure 4.

It is reported in literature that there were several cases which revealed that E_{HOMO}, E_{LUMO} and ΔE_{L-H} did not show direct correlation between these computed quantum chemical values and inhibition efficiencies determined experimentally [42]. It has been observed that lower the ΔE_{MBG} of inhibitor, higher is the corrosion inhibition efficiency. However, in present study we have found that in addition to ΔE_{MBG}, E_{HOMO} and ΔE_{H-L} show direct correlation with inhibition efficiencies obtained experimentally (Table 5).

Table 5. Calculated quantum chemical parameters for different Mannich bases

Inhibitor	**E_{HOMO}**	**E_{LUMO}**	**EA**	**ΔE_{H-L}**	**ΔE_{MBG}**	***η**	**ΔN**
	(eV)	**(eV)**	**(eV)**	**(eV)**	**(eV)**	**%**	
M-1	-6.148	-2.451	-1.119	3.697	1.815	94.8	0.731
M-2	-6.162	-2.465	-1.192	3.696	1.817	91.4	0.727
M-3	-6.121	-2.429	-1.143	3.691	1.812	96.2	0.738

It is understood from literature that the higher the HOMO energy (E_{HOMO}) of the inhibitor, the greater tendency to offer electrons to unoccupied d orbital of the metal, and the higher the corrosion inhibition efficiency. Table 5 shows that E_{HOMO} of studied Mannich bases increased in the order: M-2 < M-1 < M-3; ΔE_{L-H} decreased in order: M-2 > M-1 > M-3 and ΔE_{MBG} decreased in the order: M-2 > M-1 > M-3. The values of E_{HOMO}, ΔE_{L-H} and ΔE_{MBG} are correlated to inhibition efficiencies determined experimentally for three Mannich bases. These observations are reinforced by the results of number of transferred electrons (ΔN) calculation.

The number of transferred electrons (ΔN) is calculated depending on the quantum chemical method using the following equation:

$$\Delta N = \frac{(\chi_{Fe} - \chi_{inh})}{2(\eta_{Fe} + \eta_{inh})}$$

where χ_{Fe} and χ_{inh} denote the absolute electronegativity of iron and the inhibitor molecule, respectively; η_{Fe} and η_{inh} denote the absolute hardness of iron and the inhibitor molecule, respectively. These quantities are related to electron affinity (A) and ionization potential (I) as follows:

$$\chi = \frac{I + A}{2}; \qquad \eta = \frac{I - A}{2}$$

I and A are related in turn to E_{HOMO} and E_{LUMO} as follows:

$$I = -E_{HOMO}; \qquad A = -E_{LUMO}$$

Values of χ and η were calculated by using the values of I and A obtained from quantum chemical calculation. Using a theoretical χ value of 7.0 eV/mol and η value of 0 eV/mol for iron, ΔN, is the fraction of electrons transferred (electrons donated) from inhibitors to the iron surface. If ΔN < 3.6, the inhibition efficiency increases with increasing electron-donating ability at the metal surface. The calculated ΔN values for M-1, M-2 and M-3 are 0.731, 0.727 and 0.738, respectively, confirming the experimental results. Within a series of molecules, the ΔN values may show different trends however, their absolute values do not represent an exact number of electrons leaving the donor and entering the acceptor molecule.

3.5. Inhibition mechanism

The rate of adsorption is usually rapid and can occur through the replacement of solvent molecules from metal surface by ions and molecules accumulated at the metal/ solution interface [43-45]. The interactions between a metal surface and an inhibitor molecule depends on the number of heteroatom (O, N, S), benzene ring and relative coordinating strength towards the given metal [46]. According to the well accepted model, the adsorption of organic inhibitor molecules is often a displacement reaction involving removal of adsorbed water molecules from the metal surface [47, 48].

$$Org_{(sol)} + xH_2O \rightarrow Org_{(ads)} + xH_2O_{(sol)}$$

Existence of non-bonding electrons on heteroatoms, π -electrons from the aromatic rings and imine group in neutral inhibitor molecules may interact with the metal surface other than electrostatic interactions. The effectiveness of a corrosion inhibitor depends on the structure of inhibitor molecule and the variation in inhibitive efficiency mainly depends on the type and the nature of the substituents

present in the inhibitor molecule [49, 50]. Thus, on the basis of these factors, the difference in protective action of the tested Mannich bases can be explained. In the present study the inhibition efficiency value are in the order: M-3 > M-1 > M-2. In this group of three Mannich bases '3-(4-chlorophenyimino)indolin-2-one' (CPI) moiety is common and only difference is in the secondary amine. So difference in inhibitor efficiency might be due to this difference. The inhibitor M-3 showed the best performance due to the presence of di-n-butylamino group. The longer alkyl chain covered larger surface area of the metal, resulting in higher inhibition efficiency. The lower protective action of M-2 than M-1 can be attributed to the presence of morpholino group. The chair conformation of morpholino group is in such a way that CPI moiety is no longer to be planar to the mild steel surface, resulting in lesser adsorption and consequently in lower protection.

4. CONCLUSIONS

1. The adsorption of inhibitor molecules at the metal/acid solution interface occur suggested by the experimental results which inhibit corrosion of mild steel in 1M HCl solutions.
2. Electrochemical impedance spectroscopy, polarization measurements and weight loss measurement techniques gave consistent results from which we can conclude that the efficiency of four tested Mannich bases follow the order: M-3 > M-1 > M-2.
3. Thermodynamic values well supported the experimental results and the values of K_a together with free energy of adsorption ($\Delta G°_a$) support the experimental results.
4. The results of Tafel polarization curves showed that all the four Mannich bases under investigation were mixed type inhibitors.
5. Quantum chemical properties such as ΔE_{MBG}, $\Delta E_{L\text{-}H}$ and E_{HOMO} are correlated well to the experimentally determined inhibition efficiencies. It was concluded that the higher E_{HOMO}, the lower ΔE_{MBG} and the lower $\Delta E_{L\text{-}H}$ increase the inhibition efficiency.

ACKNOWLEDGEMENT
Authors are thankful for the Sichuan 1000 Talent fund, and Open Fund (PLN1411) of State Key Laboratory of Oil and Gas Reservoir Geology and Exploitation, Southwest Petroleum University, Chengdu, China.

References

1. Z. Tao, S. Zhang, W. Li, B. Hou, *Ind. Eng. Chem. Res.*, 50 (2011) 6082.
2. Z. Tao, S. Zhang, W. Li, B. Hou, *Ind. Eng. Chem. Res.*, 49 (2010) 2593.
3. I. B. Obot, N. O. Obi-Egbedi, A. O. Eseola, *Ind. Eng. Chem. Res*., 50 (2011) 2098.
4. F. Bentiss, M. Traisnel, H. Vezin, M. Lagrene, *Ind. Eng. Chem. Res.*, 39 (2000) 3732.
5. I. Ahamad, R. Prasad, M.A. Quraishi, *Mater. Chem. Phys*., 124 (2010) 1155.
6. M. Yadav, T.K. Sarkar, I.B. Obot, *Corros. Sci*., (2017) http://dx.doi.org/10.1016/j.corsci.2017.03.002.
7. A. Singh, K. R. Ansari, A. Kumar, W. Liu, C. Songsong, Y. Lin, *J. All. Comp.*, 712 (2017) 121.

8. N. Yilmaz, A. Fitoz, U. Ergun, K. C. Emregul, *Corros. Sci*., 111 (2016) 110.
9. N. Kicir, G. Tansug, M. Erbil, T. Tuken, *Corros. Sci*., 105 (2016) 88.
10. E. Kowsari, S. Y. Arman, M. H. Sahini, H. Zandi, A. Ehsani, R. Naderif, A. Pourghasemihanza, M. Mehdipour, *Corros. Sci*., 112 (2016) 73.
11. D. Zhang, Y. Tang, S. Qi, D. Dong, H. Cang, G. Lu, *Corros. Sci*., 102 (2016) 517.
12. K. R. Ansari, M. A. Quraishi, A. Singh, *Corros. Sci*., 79 (2014) 5.
13. H. Keles, D. M. Emir, M. Keles, *Corros. Sci*., 101 (2015) 19.
14. X. Li, X. Xie, S. Deng, G. Du, *Corros. Sci*., 92 (2015) 136.
15. A. Singh, Y. Lin, I. B. Obot, Eno E. Ebenso, K. R. Ansari, M. A. Quraishi, *Appl. Surf. Sci*., 356 (2015) 341.
16. I. Ahamad, R. Prasad, M. A. Quraishi, *Corros. Sci*., 52 (2010) 1472.
17. Motsie E. Mashuga, Lukman O. Olasunkanmi, Eno E. Ebenso, *J. Mol. Struc*., 1136 (2017) 127.
18. Mathiyan Muralisankar, R. Sreedharan, S. Sujith, Nattamai S.P. Bhuvanesh, A. Sreekanth, *J. All. Comp*., 695 (2017) 171.
19. Tahar Douadi, Hanane Hamani, Djamel Daoud, Mousa Al-Noaimi, Salah Chafaa, *J. Tai, Inst, chem., engg*., 71 (2017) 388.
20. J. Z. Ai, X.P. Guo, J.E. Qu, Z.Y. Chen, J.S. Zheng, *Colloids Surf. A: Physicochem. Eng. Asp.,* 281 (2006) 147.
21. O. K. Abiola, *Corros. Sci*., 48 (2006) 3078.
22. V.S. Sastri, J.R. Perumareddi, *Corros.*, 53 (1997) 617.
23. Bereket, G.; Ogretir, C.; Ozsahin, *C. J. Mol. Struct. (Theochem),* 663 (2003) 39 .
24. I.B. Obot, N.O. Obi-Egbedi, A.O. Eseola, *Ind. Eng. Chem. Res*., 50 (2011) 2098.
25. I. Ahamad, R. Prasad, M. A. Quraishi, *Corros. Sci*., 52 (2010) 1472.
26. Gaussian 03, M. J. Frisch, G. W. Trucks, H. B. Schlegel, G. E. Scuseria, M. A. Robb, J. R. Cheeseman, J. A. Montgomery, Jr., T. Vreven, K. N. Kudin, J. C. Burant, J. M. Millam, S. S. Iyengar, J. Tomasi, V. Barone, B. Mennucci, M. Cossi, G. Scalmani, N. Rega, G. A. Petersson, H. Nakatsuji, M. Hada, M. Ehara, K. Toyota, R. Fukuda, J. Hasegawa, M. Ishida, T. Nakajima, Y. Honda, O. Kitao, H. Nakai, M. Klene, X. Li, J. E. Knox, H. P. Hratchian, J. B. Cross, V. Bakken, C. Adamo, J. Jaramillo, R. Gomperts, R. E. Stratmann, O. Yazyev, A. J. Austin, R. Cammi, C. Pomelli, J. W. Ochterski, P. Y. Ayala, K. Morokuma, G. A. Voth, P. Salvador, J. J. Dannenberg, V. G. Zakrzewski, S. Dapprich, A. D. Daniels, M. C. Strain, O. Farkas, D. K. Malick, A. D. Rabuck, K. Raghavachari, J. B. Foresman, J. V. Ortiz, Q. Cui, A. G. Baboul, S. Clifford, J. Cioslowski, B. B. Stefanov, G. Liu, A. Liashenko, P. Piskorz, I. Komaromi, R. L. Martin, D. J. Fox, T. Keith, M. A. Al-Laham, C. Y. Peng, A. Nanayakkara, M. Challacombe, P. M. W. Gill, B. Johnson, W. Chen, M. W. Wong, C. Gonzalez, and J. A. Pople, Gaussian, Inc., Wallingford CT, 2004.
27. I. Ahamad, R. Prasad, M. A. Quraishi, *Corros. Sci*., 52 (2010) 3033.
28. M. Bouklah, B. Hammouti, M. Lagrenee, F. Bentiss, *Corros. Sci*., 48 (2006) 2831.
29. Z. Tao, S. Zhang, W. Li, B. Hou, *Corros. Sci.*, 51 (2009) 2588.
30. Zhihua Tao, Shengtao Zhang, Weihua Li, Baorong Hou, *Ind. Eng. Chem. Res.*, 50 (2011) 6082.
31. C. Jeyaprabha, S. Sathiyanarayanan, G. Venkatachari, *Appl. Surf. Sci*., 253 (2006) 432.
32. Y. Tang, X. Yang, W. Yang, R. Wan, Y. Chen, X. Yin, *Corros. Sci.*, 52 (2010) 1801.
33. K. F. Khaled, M. M. Al-Qahtani, *Mater. Chem. Phys*., 113 (2009) 150.
34. G. Avci, *Colloids Surf. A*, 317 (2008) 730.
35. M. A. Quraishi, A. Singh, V. K. Singh, D. K. Yadav, A. K. Singh, *Mater. Chem. Phys.,* 122 (2010) 114.
36. A. Singh, Y. Lin, W. Liu, S. Yu, J. Pan, C. Ren, D. Kuanhai, *J. Ind. Engg. Chem*., 24 (2015) 219.
37. A. Singh, I. Ahamad, V. K. Singh, M. A. Quraishi, *J. Solid State Electrochem.*, 15 (2011) 1087.
38. A. Singh, Y. Lin, W. Liu, D. Kuanhai, J. Pan, B. Huang, C. Ren, D. Zeng, *J. Tai. Inst. Chem. Eng.*, 45 (2014) 1918.
39. A. Singh, I. Ahamad, M. A. Quraishi, *Arab. J. Chem.*, 9 (2012) S1584.

40. A. Singh, Y. Lin, W. Liu, J. Pan, B. Huang, *J. Ind. Engg. Chem*., 20 (2014) 4276.
41. D. K. Yadav, M. A. Quraishi, B. Maiti, *Corros. Sci.,* 55 (2012) 254.
42. A. Singh, Y. Lin, K. R. Ansari, M. A. Quraishi, Eno. E. Ebenso, S. Chen, W. Liu, *Appl. Surf. Sci*., 359 (2015) 331.
43. Ambrish Singh, Yuanhua Lin, I.B. Obot, Eno. E. Ebenso, L. Mol. Liq., 219 (2016) 865.
44. D. K. Yadav, D. S. Chauhan, I. Ahamad, M. A. Quraishi, *RSC. Adv.,* 3 (2013) 632.
45. K.R. Ansari, M.A. Quraishi, Ambrish Singh, *J. Ind. Engg. Chem*., 25 (2015) 89.
46. J. Fang, J. Li, *J. Mol. Struct. (Theochem),* 593 (2002) 179.
47. G. Bereket, E. Hur, C. Ogretir, *J. Mol. Struct. (Theochem*), 578 (2002) 79.
48. L. Tang, X. Li, L. Li, G. Mu, G. Liu, *Mater. Chem. Phys*., 97 (2006) 301.
49. G. Moretti, F. Guidi, G. Grion, *Corros. Sci*., 46 (2004) 387.
50. I. M. Ritchie, S. Bailey, R. Woods, *Adv. Colloid Interface Sci*., 80 (1999) 183.